The genetic basis of hindwing eyespot number variation in *Bicyclus anynana* butterflies

Angel G. Rivera-Colón[*, †], Erica L. Westerman[‡], Steven M. Van Belleghem[†], Antónia Monteiro[§,**], and Riccardo Papa[†]

Affiliations

*Department of Animal Biology, University of Illinois, Urbana-Champaign

†University of Puerto Rico-Rio Piedras Campus

‡University of Arkansas, Fayetteville

§National University of Singapore

**Yale-NUS College

Data accessibility

The *Bicyclus anynana* PstI RAD-tag sequencing data is available via the Genbank Bioproject PRJNA509697. Genotype VCF files will be made available through figshare upon acceptance.

18 **Running Title:** Genetics of eyespot number variation

19

20 **Key words:** Serial homology, genetics, *apterous*, eyespot number, *Bicyclus anynana,*

21 genetic architecture

22

23 **Co-Corresponding Authors:**

24 antonia.monteiro@nus.edu.edu and rpapa.lab@gmail.com

Abstract

The underlying genetic changes that regulate the appearance and disappearance of repeated traits, or serial homologs, remain poorly understood. One hypothesis is that variation in genomic regions flanking master regulatory genes, also known as input-output genes, controls variation in trait number, making the locus of evolution almost predictable. Other hypotheses implicate genetic variation in up-stream or downstream loci of master control genes. Here, we use the butterfly *Bicyclus anynana*, a species which exhibits natural variation in eyespot number on the dorsal hindwing, to test these two hypotheses. We first estimated the heritability of dorsal hindwing eyespot number by breeding multiple butterfly families differing in eyespot number, and regressing eyespot number of offspring on mid-parent values. We then estimated the number and identity of independent genetic loci contributing to eyespot number variation by performing a genome-wide association study with restriction site-associated DNA Sequencing (RAD-seq) from multiple individuals varying in number of eyespots sampled across a freely breeding lab population. We found that dorsal hindwing eyespot number has a moderately high heritability of approximately 0.50. In addition, multiple loci near previously identified genes involved in eyespot development display high association with dorsal hindwing eyespot number, suggesting that homolog number variation is likely determined by regulatory changes at multiple loci that build the trait and not by variation at single master regulators or input-output genes.

Introduction

Body plans often evolve through changes in the number of repeated parts or serial homologs by either addition or subtraction. For instance, the pelvic fins of vertebrates are inferred to have originated after the appearance of pectoral fins, perhaps via co-option of the pectoral or caudal fin developmental programs to a novel location in the body (Larouche, Zelditch, & Cloutier, 2017; Ruvinsky & Gibson-Brown, 2000). In insects, the absence of limbs and wings in the abdomen is inferred to be due to the repression (or modification) of limbs and wings in these segments by *hox* genes (Galant & Carroll, 2002; Ohde, Yaginuma, & Niimi, 2013; Ronshaugen, McGinnis, & McGinnis, 2002; Tomoyasu, Wheeler, & Denell, 2005). Regulatory targets of abdominal *hox* genes are likely to underlie loss of limb/wing number in these body segments (Ohde et al., 2013; Tomoyasu et al., 2005), although these mutations have not yet been identified. Thus, while serial homolog number variation is a common feature in the evolution of organisms' body plans, the underlying genetic changes that regulate the appearance and disappearance of these repeated traits remain poorly understood.

Studies in *Drosophila* have contributed most to the identification of the genetic basis underlying the evolution of serial homolog number. Larvae of different species have different numbers of small hairs, or trichomes, in their bodies, and variation in regulatory DNA around the gene *shavenbaby* appears to be largely responsible for this variation (McGregor et al., 2007). Moreover, *shavenbaby* has been labeled a master regulatory gene because its ectopic expression in bare regions of the body leads to

trichomes (Payre, Vincent, & Carreno, 1999). However, a more complex genetic architecture seems to underlie variation in the number of larger bristles found in the thorax of adults. In this case variation around *achaete-scute*, a gene complex required for bristle differentiation, plays a role in controlling bristle number variation across species (Marcellini & Simpson, 2006). Interestingly, genetic variation in upstream regulatory factors, whose spatial expression overlaps some, but not all bristles, is also known to impact bristle number in lab mutants (Garcia-Bellido & de Celis, 2009). Finally, *shavenbaby* and *scute* genes are also known as input-output genes due to their central "middle of the hour-glass" position in regulatory networks (Stern & Orgogozo, 2008). These genes respond to the input of multiple upstream protein signals, present at distinct locations in the body, and in turn control the regulation of the same battery of downstream genes, to affect the same output (trichome or bristle development) at each of these body locations. Mutations in the regulatory regions of these genes are thus expected to have minimal pleiotropic effects, and to lead to changes in the number of times the network is deployed, and thus to evolution in the number of trichome or bristles in the bodies of these flies. While this type of regulatory network architecture points to predictable regions in the genome that will readily evolve leading to trait number evolution, i.e., hotspots of evolution, it might represent only one type of architecture among others that are still unexplored. More systems, thus, need to be investigated for a more thorough understanding of the genetic basis underlying variation of repeated traits in bodies.

One promising system for investigating the genetic basis of serial homolog number evolution are the eyespot patterns on the wings of nymphalid butterflies. Eyespots originally appeared on the ventral hindwing in a lineage of nymphalid butterflies, sister to the Danainae, and have subsequently been added to the forewings and dorsal surfaces of both wings (Oliver, Beaulieu, Gall, Piel, & Monteiro, 2014; Oliver, Tong, Gall, Piel, & Monteiro, 2012; Schachat, Oliver, & Monteiro, 2015). Furthermore, within a single species, eyespot number can vary significantly between individuals or sexes (Brakefield & van Noordwijk, 1985; Owen, 1993; Tokita, Oliver, & Monteiro, 2013), allowing for population genetic approaches to identify the underlying genetic basis of such variation. Genes controlling eyespot number variation within a species might also be involved in promoting this type of variation seen across species.

One of the best model species for studying the genetic basis of eyespot number variation is the nymphalid butterfly *Bicyclus anynana*. This species exhibits natural variation and sexual dimorphism in eyespot number on the dorsal hindwing surface, which play a possible role in mate choice (Westerman, Chirathivat, Schyling, & Monteiro, 2014). The observed variation consists of males averaging 0.75 dorsal hindwing eyespots, with a range of 0-3, and females averaging 1.5 dorsal hindwing eyespots, with a range of 0-5 (Westerman et al., 2014) (Fig. 1). Lab populations of this species also display a series of mutant variants that affect eyespot number on other wing surfaces. Genetic and developmental studies on eyespot number variation in this species suggest the existence of at least two different underlying molecular mechanisms. Spontaneous mutants such as Spotty (Brakefield & French, 1993;

Monteiro et al., 2013; Monteiro, Brakefield, & French, 1997), Missing (Monteiro et al., 2007), P- and A- (Beldade, French, & Brakefield, 2008), or X-ray induced mutations such as 3+4 (Monteiro, Prijs, Bax, Hakkaart, & Brakefield, 2003), segregate as single Mendelian alleles, and cause discrete and obvious changes in eyespot number or affect the size of very specific eyespots. On the other hand, multiple alleles of small effect likely regulate the presence or absence of small eyespots that sometimes appear between the typical two eyespots on the forewing, or on the most posterior wing sector of the ventral hindwing. This type of eyespot number variation is positively correlated with eyespot size variation, responds readily to artificial selection on eyespot size (Beldade & Brakefield, 2003; Holloway, Brakefield, & Kofman, 1993; Monteiro, Brakefield, & French, 1994), and is likely under the regulation of a threshold type mechanism (Brakefield & van Noordwijk, 1985).

Interestingly, eyespot number variation within *B. anynana* can involve changes to single eyespots or to several eyespots at a time, on one or both wing surfaces. For instance, Spotty introduces two eyespots on the dorsal and ventral surfaces of the forewing, whereas A- and P- primarily reduce the size of the single anterior (A-) or the posterior eyespot (P-) of the dorsal surface exclusively, without affecting eyespot size or number on the ventral surface. The genetic basis for these differences is still unknown.

Recently, the gene *apterousA* (*apA*) was shown to regulate wing pattern differences between dorsal and ventral surfaces in *B. anynana*, including differences in eyespot

number (Prakash & Monteiro, 2018). This gene is expressed exclusively on the dorsal wing surfaces and its mutation via CRISPR-Cas9 led to dorsal wing surfaces acquiring a ventral identity, which included additional eyespots. This study indicated that *apA* is a repressor of eyespots on the dorsal surface. However, *B. anynana*, has eyespots on dorsal wing surfaces and their presence and variation in number appears to be correlated with variation in the number of small circular patches, positioned at future eyespot centers, lacking *apA* expression (Prakash & Monteiro, 2018). This suggests that genetic variation at loci that modulate the expression of *apA* in eyespot centers on the dorsal surface, or genetic variation in regulatory regions of *apA* itself, might be involved in regulating eyespot number specifically on the dorsal surface of wings.

The genetic architecture of eyespot number variation in any butterfly species remains unknown. Here, we examine the genetic basis of dorsal hindwing eyespot number (DHEN) variation in *B. anynana*. We carried out two sets of experiments. We first estimated the heritability for this trait by breeding multiple butterfly families differing in eyespot number and regressing eyespot number of offspring on mid-parent values. Then we estimated the number and identity of independent genetic loci that are contributing to variation in this trait by performing a genome-wide association study with restriction site-associated DNA Sequencing (RAD-seq) from multiple individuals varying in number of eyespots sampled across a freely breeding lab population.

Materials and Methods

Study organism

Bicyclus anynana is a Nymphalid butterfly common to sub-tropical Africa for which a colony has been maintained in the laboratory since 1988. All *Bicyclus anynana* butterflies used in this study were collected from a colony established in New Haven, CT (Yale University), composed of an admixed population of numerous generations of freely breeding individuals with variable dorsal hindwing eyespot number phenotypes. Individuals from this colony originated from an artificial colony established in Leiden University in 1988, which was established from numerous gravid females collected in Malawi in 1988. Previous studies have estimated that this laboratory population maintains genetic diversity comparable to those of natural populations (reviewed in Westerman et al., 2016). The colony was kept in controlled conditions of 12 hours light/dark cycles, 80% relative humidity and a temperature of 27^{o}C. Larvae were fed on corn plants and adult butterflies on mashed banana, as described in previous publications (Westerman et al., 2014).

Heritability of dorsal hindwing eyespot number

We examined the number of dorsal hindwing eyespots (DHEN) on all offspring from 18 separately reared families whose parents differed in eyespot number: six families where both parents had DHEN of zero (0F x 0M); six where both parents had DHEN of one (1F x 1M); and six where both parents had DHEN of two (2F x 2M). All generations were reared in the conditions described above. We ensured virginity of

the females by separating the butterflies in the parental generation into sex-specific cages on the day of eclosion. All families were started within 5 days of each other using adults ranging from 1-3 days old (ANOVA, n=18, DF=2, F=0.8266, p=0.4565). Each breeding pair was placed in a cylindrical hanging net cage of 30 cm diameter X 40 cm height, with food (banana slices), water and a young corn plant on which to lay eggs. When corn plants were covered with eggs, they were placed in family-specific mesh sleeve cages for larval growth. Females were given new plants on which to lay eggs until they died. Pupae and pre-pupae were removed from the sleeve cages and placed in family-specific cylindrical hanging net cages for eclosion. The cages were checked daily for newly emerged butterflies. On the day of eclosion, DHEN was recorded for each offspring. Heritability was calculated by regressing offspring on midparent values, correcting the estimate for assortative mating, as described in Falconer & Mackay (1996). Estimates were obtained for the pooled offspring data as well as for separate regressions of female and male offspring data on mid-parent values. Sex-specific heritabilities were calculated using the correction for unequal variances in the two sexes (Falconer and Mackay, 1996). We then tested for an interaction of parental phenotype and offspring sex on offspring phenotype using a general linear model, with sex, parental phenotype, and sex*parental phenotype as fixed variables.

Sample collection and phenotype determination for genomic association study

To identify regions in the genome that are associated with DHEN variation, we collected and sequenced a total of 30 individuals. Fifteen individuals contained no

eyespots (absence) and 15 containing two or more eyespots (presence) (Table S1). Both groups contained an assorted number of male and female individuals. Wings of the collected individuals were removed, and the bodies were preserved in ethanol for DNA extraction.

RAD library preparation and sequencing

Genomic DNA of the preserved bodies was extracted using DNeasy Blood & Tissue Kit (Qiagen), with an additional RNase digestion for removing RNA from the extracted nucleic acid samples. The quality and concentration of the extracted DNA was verified using gel electrophoresis and Qubit 2.0 fluorometer (Life Technologies). Extracted genomic DNA was used for preparing Illumina RAD sequencing libraries based on previously described protocols (Baird et al., 2008; Etter, Bassham, Hohenlohe, Johnson, & Cresko, 2011). DNA was digested with the frequent cutting enzyme *Pst*1 and ligated to P1 adapters containing a unique barcode 5 bp in length. Samples were pooled and sheared using a Covaris M220 (Covaris Inc.) instrument and size selected for 300-500 bp inserts on average. After end-repair and P2 adapter ligation, the library was amplified by PCR. The pooled library was then sequenced utilizing a single lane of an Illumina HiSeq2000® 100 bp paired-end module.

Read quality and filtering

Following sequencing of a RAD-seq library composed of 30 *B. anynana* individuals, we obtained 127 million paired-end reads 100 bp in length. The raw RAD reads were demultiplexed using *Stacks v1.42* (Catchen, Hohenlohe, Bassham, Amores, & Cresko,

2013; Catchen et al., 2011) *process_radtags* pipeline, and reads with low quality and/or ambiguous barcodes were discarded. Further, we removed Illumina adapter sequences from the reads and trimmed sequences to 80 bp in length, as suggested from the FastQC quality control tool (http://www.bioinformatics.babraham.ac.uk/projects/fastqc/) results. We retained a total of 111 million (86 %) and an individual average of 3.7 million ± 1.2 million filtered paired-end reads.

Reference alignment

The 111 million retained read pairs were aligned to the most recent *B. anynana* genome assembly (v1.2) with its corresponding annotation (Nowell et al., 2017). This reference assembly is composed of 10,800 individual scaffolds, for a total genome size of about 475 Mb (N50 = 638.3 kb). The annotation contains 22,642 genes, with a partial CEGMA completeness of 97.2 %. Filtered reads were aligned to the reference genome using BWA v0.7.13 (H. Li & Durbin, 2009) *mem* with default seed lengths, mismatch and gap scores, but allowing for the marking of shorter split reads as secondary alignments for compatibility with PicardTools v1.123 (https://broadinstitute.github.io/picard/). Resulting alignments were directly converted to BAM files using SamTools v1.12 (H. Li et al., 2009) *view*. BAM files were then sorted with SamTools *index* and filtered for duplicates using PicardTools v1.123 *MarkDuplicates* and processed with *AddOrReplaceReadGroups* for GATK compatibility. In total, we obtained a 92.9 % read alignment and 79.6 % properly

mapped read pairs. At each RAD locus, average per-individual sequencing coverage was 18.8X (± 4.3; median: 18.3).

Variant calling and association mapping

Identification of associated regions of the genome was performed simultaneously using two different analytical approaches to produce method-agnostic results. The first one, referred to as the "association method", identified variants on the filtered BAM files using GATK v3.5 (McKenna et al., 2010) *UnifiedGenotyper* with the default call confidence values and outputting only variant sites. These variant sites were then filtered using VCFTools v0.1.14 (Danecek et al., 2011) *recode* to obtain only calls with a minimum genotype quality of 30, a minimum genotype depth of 5, present in over 50 % of all individuals, a max allele number of 2, and minimum allele frequency of 0.05. This results in a filtered VCF containing only high-quality biallelic variants. After genotyping with *GATK*, we obtained 350,121 filtered SNPs. Genotype-to-phenotype association in the genotyped samples via the "association method" was performed using PLINK v1.90 (Clarke et al., 2011; Purcell et al., 2007). We used a genome-wide adjusted Fisher analysis to identify genotype-to-phenotype association values for each SNP. The test also implements an adaptive Monte Carlo permutation analysis to reduce the detection of false positives. This process tests the obtained *p*-values per locus after each successive permutation, with a maximum of 1,000,000 replications.

The second analytical approach, referred to as the "F_{ST} method", called SNPs using Stacks v1.42. Using the *ref_map.pl* wrapper script with default parameters, RAD loci were assembled from the reference genome-mapped reads using *pstacks*. A catalog of

all loci was generated with *cstacks* and samples were matched to this catalog using *sstacks.* The *populations* program was then run on this catalog to generate population genetic measures, enabling the calculation of F-statistics. For a variant to be included in the analysis, it had to be present in both study groups in over 75% percent of individuals (p=2, r=0.75) and have a minimum allele frequency above 0.05. Additionally, a Fisher's Exact Test p-value correction was applied to the resulting F_{ST} and Analysis of Molecular Variance (AMOVA) F_{ST} values as a multiple testing correction. Using *Stacks* for the F_{ST} method we reconstructed 207,752 RAD loci and 673,340 raw SNPs. After filtering, 73,159 RAD loci and 238,786 SNPs were retained. Filtered variants obtained from both datasets were compared to retain only SNPs with support from both genotyping methods. A total of 216,338 SNPs were shared between the two datasets and were used for subsequent comparisons.

Selection of candidate loci

To minimize the identification of false genotype-to-phenotype relationships, only areas of the genome displaying both association and F_{ST} peaks were used for further analysis. The use of both metrics simultaneously also ensured that the relationships observed are method agnostic. This multi-metric approach, including a combination of association and F_{ST} outliers, has been utilized repeatedly to identify genomic regions associated with domestication in both dogs and cats (Axelsson et al., 2013; Montague et al., 2014), variation in feather coloration in warblers (Brelsford, Toews, & Irwin, 2017), and the architecture and modularity of wing pattern variation in *Heliconius* butterflies (Nadeau et al., 2014; Van Belleghem et al., 2017). Significant

295 peaks were defined as areas of the genome with SNPs containing association and/or
296 F_{ST} 10 standard deviations above the genome-wide mean. Candidate variants were
297 then annotated using *SnpEff* v4.3T (Cingolani et al., 2012), building a *de novo* database
298 with the available *B. anynana* reference annotation, to identify possible effects over
299 nearby genes.
300
301 **Principal Component Analysis**
302 To determine the baseline-level genome-wide diversity and divergence among
303 individuals in the present population, we performed a Principal Component Analysis
304 (PCA) on the obtained genotypes. Although our sampled individuals originated from
305 a single, freely breeding population, performing this analysis allowed us to
306 corroborate that the observed genomic diversity lacks any substructuring that could
307 impact our outlier identification. To do this, we randomly selected a subset of 5000
308 filtered variants from the *Stacks* catalog and made them into a whitelist, as described
309 by the *Stacks* manual and by Rochette & Catchen (2017). We then ran the *populations*
310 module on this subset of variants with the addition of the --*genepop* export format
311 flag. The resulting genepop file was processed using the *adegenet* v2.1.1 R package
312 (Jombart, 2008; Jombart & Ahmed, 2011) by converting the genotype calls into a
313 *genind* object, scaling missing data by mean allele frequency and analyzed with PCA.
314
315 **Ordering of the *B. anynana* scaffolds along the *Heliconius melpomene* genome**
316 The current *B. anynana* reference assembly (Nowell et al., 2017) has an N50 of 638.3
317 kb and is composed of 10,800 unlinked scaffolds. To assess whether associated SNPs

318 on separate *B. anynana* genome scaffolds could be part of the same block of
319 association, we ordered the scaffolds of the *B. anynana* genome along the *Heliconius*
320 *melpomene* v2 genome assembly (Davey et al., 2016). Although *B. anynana* and *H.*
321 *melpomene* diverged about 80 My ago (Espeland et al., 2018) and have a different
322 karyotype (n=28 in *B. anynana* versus n=21 in *H. melpomene*), the *H. melpomene*
323 genome is the most closely related butterfly genome that has been assembled into
324 highly contiguous chromosomal scaffolds using pedigree informed linkage maps.
325 Aligning both genomes provides valuable information to interpret our association
326 analysis. To construct this alignment, we used the alignment tool *promer* from the
327 MUMmer v3.0 software suite (Kurtz et al., 2004). *Promer* was used with default
328 settings to search for matches between sequences translated in all six possible
329 reading frames between the *B. anynana* and *H. melpomene* genome. The obtained
330 alignments were subsequently filtered for a minimum alignment length of 200 bp and
331 a minimum percent identity (%IDY = (matches x 100)/(length of aligned region)) of
332 90 %. These filtered alignments were used to order the *B. anynana* scaffolds according
333 to the order in which they aligned along the *H. melpomene* genome. If a scaffold
334 aligned to multiple locations or chromosomes, priority was given to the position it
335 matched with highest identity. For scaffolds that contained significant associations
336 with hindwing eyespot number, we also retained alignments with a minimum %IDY
337 of 70 % and a minimum alignment length of 150 bp to investigate possible fine scale
338 rearrangements between the *B. anynana* and *H. melpomene* genome.
339
340

341 **Linkage disequilibrium analysis**

342 In addition to ordering the *B. anynana* scaffolds to the *H. melpomene* genome for
343 assessing the genomic linkage of SNPs, we calculated linkage disequilibrium in our *B.*
344 *anynana* study population. To calculate linkage disequilibrium for genomic SNPs, we
345 phased 213,000 SNPs that were genotyped in all samples using *beagle* v4.1 (Browning
346 & Browning, 2007). Estimates of linkage disequilibrium were calculated from
347 100,000 randomly selected SNPs, using the *VCFtools* v0.1.14 (Danecek et al., 2011) –
348 *hap-r2* function, with a max LD window of 5 Mbp, and minimum allele frequency
349 cutoff of 0.10. Resulting LD comparisons for genomic SNPs were then plotted in R,
350 where a Loess local regression was calculated and used to determine the genome-
351 wide window size of linkage disequilibrium decay. Subsequently, this LD window size
352 was used for the investigation of genes near associated loci.

353

354 **Results**

355

356 **Dorsal hindwing spot number variation has moderate to high heritability**

357 Zero spot females were only produced by 0x0 families and one 1x1 family, and were
358 absent from any 2x2 DHS families. Zero spot males, however, were produced by all
359 0x0 families, all but one of the 1x1 families and all but one of the 2x2 families. Two
360 spot females were produced by all but one (a 0x0) family, while 2 spot males were
361 produced by all 2x2 families, but only two 1x1 families and one 0x0 family (Table 1).
362 These results demonstrate that alleles are sufficiently segregating in our
363 experimental design to perform heritability estimates.

DHEN has a heritability of 0.4442 ± 0.264 for females, 0.5684 ± 0.306 for males, and 0.5029 ± 0.159 when the sexes were pooled. There was no significant interaction of parental phenotype and offspring sex on offspring phenotype (General linear Model with sex, parental phenotype, and sex*parental phenotype as parameters, AICc (Akaike Information Criterion) = 1498.204, effect tests: sex χ^2=293.361, p<0.0001; parental phenotype χ^2=271.56, p<0.0001; sex* parental phenotype χ^2=0.032, p=0.8576).

Genome-wide variation and linkage disequilibrium of the study population

To confirm the absence of population substructure in our study population, we calculated measures of genetic variation and diversity between the samples displaying presence of DHEN (pre) and samples with absent DHEN (abs). As expected, the two groups showed very little genome-wide genetic divergence, with a genome-wide F_{ST} equal to 0.0075. The absence of any population substructure between the two sampled phenotype groups was further demonstrated by complete overlap of the two groups in the PCA as well as little contribution of phenotype group to the observed variation in first and second Principal Components (Fig. 2A). Additionally, we observed very similar genome-wide nucleotide diversity in the group displaying presence of DHEN (pre, π = 0.0090) when compared to the group with absent DHEN (abs, π = 0.0083). Hence, we do not observe any demographic substructuring of the study population that could potentially bias our genetic association analysis.

After calculating genome-wide estimates of linkage disequilibrium decay (Fig. 2B), we observed a max smoothed r^2 value of 0.272, and a halving of r^2 within 464 Kb (Fig. 2B). This window size suggests that average linkage blocks are around 500 Kb in length, and that variants within this distance are in strong linkage disequilibrium.

Association mapping of dorsal hindwing spot number variation.

After mapping and genotyping RAD loci across the *B. anynana* reference (Nowell et al., 2017), we identified a total of 216,338 SNPs shared between the two different genotyping strategies used (see methods), of which 340 SNPs display both elevated F_{ST} and significantly high association with DHEN variation. These candidate SNPs are located in 15 different scaffolds of the *B. anynana* genome assembly spanning 3.54 Mbp equal to 0.744% of the whole genome (Fig. 3). The relatively close proximity of associated variants within the 15 associated scaffolds, particularly within our 500 kb LD windows, suggests that only 15 discrete regions influence DHEN variation. Further ordering these scaffolds along the contiguously assembled *Heliconius melpomene* genome suggest that they likely belong to 10 to 11 different genomic regions in the genome (Fig. 4) and thus strongly suggest DHEN variation is a polygenic trait with multiple loci.

Candidate gene identification

Using the available Lepbase reference annotation for the *B. anynana* v1.2 assembly we identified the neighboring annotated genes and relative positioning of the 340

410 outlier SNPs common to both the F_{ST} and genome-wide association. The majority of
411 these SNPs were in non-coding sequence, with 116 (34.1%) being intergenic, 78
412 (22.9%) immediately upstream, and 49 (14.4%) immediately downstream of
413 annotated genes (Supplemental Table S3). Of the 340 outlier SNPs, 11 (3.2%) produce
414 non-synonymous changes to coding regions, while 1 (0.3%) causes change in a splice
415 region sequence.
416
417 When the annotation is observed at a genic level, the biggest proportion of SNPs occur
418 closely downstream or upstream of annotated genes, 10 (23.8%) and 12 (28.6%)
419 genes, respectively, and could have regulatory effects over nearby genes
420 (Supplemental Table S3). The 11 SNPs that cause non-synonymous changes are
421 located within only two genes: 1) BANY.1.2.g01110 (Zinc finger CCCH domain-
422 containing protein 10, *ZC3H10*) has a Serine to Cysteine substitution in position 114,
423 and a Isoleucine to Valine substitution in position 142. 2) BANY.1.2.g04901
424 (Geranylgeranyl pyrophosphate synthase, *GGPS1*) contains a Arginine to Glutamine
425 substitution, and a Isoleucine to Threonine substitution in positions 96 and 98,
426 respectively. Finally, BANY.1.2.g13875 (Acidic fibroblast growth factor intracellular-
427 binding protein, *Fibp*), contains the identified splice region variant.
428
429 A number of annotated genes observed within or nearby associated regions of the
430 genome were implicated in eyespot development in previous studies, whereas other
431 genes are here implicated for the first time (Table 2). BANY.1.2.g00030 (Neutral
432 Ceramidase, *CDase*) was previously identified as differentially expressed in eyespots

433 relative to flanking wing tissue (Özsu & Monteiro, 2017). BANY.1.2.g04910 (Protein
434 spaetzle, *spz*) is involved in the regulation of the Toll signaling pathway, recently
435 implicated in eyespot development (Özsu & Monteiro, 2017). Calcium signaling-
436 related genes were also identified, including BANY.1.2.g00659 (Calcium/calmodulin-
437 dependent protein kinase type 1, *cmk*-1), BANY.1.2.g04904 (Calcium-activated
438 potassium channel slowpoke, *slo*) and BANY.1.2.g05412 (Transient receptor
439 potential channel pyrexia, *pyx*). Calcium signaling has been recently associated with
440 eyespot formation in *B. anynana* (Özsu & Monteiro, 2017). BANY.1.2.g10819 (Ero1-
441 like protein, *Ero1L*), BANY.1.2.g00658 (Disks large 1 tumor suppressor protein, *dlg1*)
442 and BANY.1.2.g00681 (Protein numb, *numb*) have functions related to Notch
443 signaling, a pathway previously associated with eyespot formation (Reed & Serfas,
444 2004). Additionally, BANY.1.2.g02571 (Homeotic protein antennapedia, *Antp*) known
445 to be expressed in early stages of eyespot development (Saenko, Marialva, & Beldade,
446 2011) and BANY.1.2.g00653 (Protein decapentaplegic, *dpp*) expressed in dynamic
447 patterns during eyespot center formation during the larval stage (Connahs et al., 2017
448 - *bioRxiv*; Monteiro, Glaser, Stockslager, Glansdorp, & Ramos, 2006) were also
449 identified within areas of high association. BANY.1.2.g04715 (C2 domain-containing
450 protein 5, *C2CD5*) appears to be involved in insulin receptor signaling, a pathway that
451 has, so far, not been implicated in eyespot development nor eyespot plasticity.

Discussion

The use of population genomic analyses, including association mapping, GWAS, and F_{ST} scans, has been extensively used in natural populations to identify the genomic components underlying a number of biological processes such as hybridization and speciation, local adaptation, and ecological and landscape genomics (Reviewed in Campbell, Poelstra, & Yoder, 2018; Narum, Buerkle, Davey, Miller, & Hohenlohe, 2013; Rellstab, Gugerli, Eckert, Hancock, & Holderegger, 2015). In our work, we applied a population genomics approach to identifying the genetic component of dorsal hindwing number variation in the butterfly *B. anynana* via the comparison of genomic diversity between individuals from a single laboratory-maintained, free-breeding population. We demonstrated that free-breeding in the laboratory population has likely maintained homogenization of the genetic variation across the genome due to a lack of demographic substructuring, reducing the detection of false positive associations between SNPs and the trait of interest, DHEN variation.

The combined results of our heritability and genome-wide association study suggest that variation in dorsal hindwing eyespot number in *B. anynana* is a complex trait regulated by multiple loci. Using a combination of RAD sequencing and genome-wide association mapping, we identified 10 to 11 potentially distinct genomic regions in the *B. anynana* reference genome associated with variation in DHEN. Further analysis of these genomic regions highlights a total of 15 candidate genes (Table 2). Some (7) of these genes have previously been found associated with eyespot development via

475 their expression patterns or via functional studies, while others (8) are suggested for
476 the first time. Complete list of all annotated genes identified in the associated regions
477 is provided in the supplemental data (Supplemental Table S2).
478
479 **DHEN variation and known elements of the eyespot regulatory network**
480 Among our identified candidates, we observe a number of genes previously
481 implicated in eyespot development in *B. anynana*. Our analysis suggests six of the
482 genes known to be expressed in eyespots are associated with DHEN: *Ubx, Antp, Dpp,*
483 *dlg1, numb*, *Ero1L*, and *CDase*. BANY.1.2.g02579 is annotated as the hox protein
484 Ultrabithorax (*Ubx*), an important selector gene that gives insect hindwings, including
485 those of butterflies, a different identity from forewings (Tong, Hrycaj, Podlaha,
486 Popadić, & Monteiro, 2014; Weatherbee et al., 1999). In *B. anynana,* this gene is
487 expressed across the whole hindwing, a conserved expression pattern observed
488 across insects, but has additional, stronger, expression in the eyespot centers of the
489 hindwing only, something that is not seen in other butterflies with eyespot such as
490 *Junonia coenia* (Tong et al., 2014). Over-expression of this gene led to eyespot size
491 reductions in both fore and hindwings of *B. anynana* (Tong et al., 2014). However,
492 absence of *Ubx* in clones of cells in the hindwing of *J. coenia* (via a spontaneous
493 unknown mutation) (Weatherbee et al., 1999) and CRISPR knockouts in *B. anynana*
494 (Y. Matsuoka, unpublished) led to both eyespot enlargements (of Cu1 eyespots to
495 sizes that match Cu1 forewing eyespot sizes), and to complete deletions of eyespots
496 that are normally present in the ventral hindwing (M2 and M3) but absent on the
497 forewing. These results suggest both a repressing role and an activating role for *Ubx*

498 that depends on eyespot position on the hindwing. Our results indicate that genetic
499 variation at *Ubx* might contribute to eyespot number variation either via a threshold-
500 like mechanism acting on eyespot size or a more discrete mechanism regulating
501 presence or absence of eyespots in specific wing sectors.
502
503 BANY.1.2.g02571 is annotated as the protein Antennapedia (*Antp*), another hox gene
504 involved in the differentiation of the anterior-posterior body axis in insects and
505 involved in the differentiation of the thoracic limbs in *Bombyx* moths (Chen et al.,
506 2013). *Antp* expression has been observed as one of the earliest expressed genes in
507 developing eyespot centers (Saenko et al., 2011), and in dorsal eyespots (Özsu &
508 Monteiro, 2017). Knock-out of *Antp* indicates this gene is required for forewing
509 eyespot development and for the development of the white centers and the full size
510 of the hindwing eyespots (Y. Matsuoka, unpublished). Variation at this locus appears
511 to contribute to hindwing eyespot number variation, perhaps using a similar
512 threshold-like mechanisms to that proposed for *Ubx*, based on eyespot size
513 regulation.
514
515 BANY.1.2.g00653 is annotated as decapentaplegic (*Dpp*), a candidate morphogen
516 likely involved in the differentiation of the eyespot centers in *B. anynana* via a
517 reaction-diffusion mechanism (Connahs et al., 2017 - *bioRxiv*). *Dpp* mRNA is
518 expressed in regions around the developing eyespots in mid to late larval wings
519 (Connahs et al., 2017 - *bioRxiv*) in anti-colocalized patterns to Armadillo, a
520 transcription factor effector of the Wingless signaling pathway, expressed in the

521 actual eyespot centers in late larval stages (Connahs et al., 2017 - *bioRxiv*). Genetic
522 variation either linked with the protein coding sequence of *Dpp*, or more likely with
523 its regulatory region affects eyespot number variation in hindwings.
524
525 Three genes known to interact with another eyespot-associated gene, *Notch* (Reed &
526 Serfas, 2004), are also implicated in our study. BANY.1.2.g00658 (Disks large 1 tumor
527 suppressor protein, *dlg1*), BANY.1.2.g00681 (protein numb, *numb*), and
528 BANY.1.2.g10819 (Ero1-like protein, *Ero1L*) are known to interact and regulate the
529 *Notch* (*N*) signaling pathway in *Drosophila melanogaster* (Cheah, Chia, & Yang, 2000;
530 Q. Li et al., 2009; Tien et al., 2008). The existence and role of these interactions are
531 unknown in *B. anynana*, as is the role of the *Notch* receptor itself. However, the *Notch*
532 receptor has a dynamic pattern of expression (Reed & Serfas, 2004) that is very
533 similar to that of *Distal-less*, a gene that has recently been implicated in setting up the
534 eyespot centers likely via a reaction-diffusion mechanism (Connahs et al., 2017 -
535 *bioRxiv*). Genetic variation at these three genes could be interacting with the eyespot
536 differentiation process through unknown mechanisms.
537
538 Newly identified components of pathways previously associated with eyespot
539 development, such as Toll and Calcium signaling (Özsu & Monteiro, 2017), have also
540 been observed among our candidates. BANY.1.2.g00959 (Calcium/calmodulin-
541 dependent protein kinase type 1, *cmk-1*), BANY.1.2.g04715 (C2 domain-containing
542 protein 5, *C2CD5*), BANY.1.2.g04904 (Calcium-activated potassium channel
543 slowpoke, *slo*) and BANY.1.2.g05412 (Transient receptor potential channel pyrexia,

544 *pyx*) all possess Calcium binding and/or interactions with Calcium signaling among
545 their annotated functions, while BANY.1.2.g00647 (Phosphoinositide 3-kinase
546 adapter protein 1, *PIK3AP1*) and BANY.1.2.g04910 (Protein spaetzle, *spz*) both
547 interact and/or regulate the Toll signaling pathway among their annotated functions.
548 *Spaetzle*, in particular, is a ligand that enables the activation of the Toll pathway in
549 *Drosophila* (Yamamoto-Hino & Goto, 2016). The role of *Spaetzle* is currently unknown
550 in the context of eyespot development but this ligand could be an interesting target
551 of further study. Our data suggests that genetic variation at these loci are also
552 regulating hindwing eyespot number variation.
553
554 **Effects of non-coding mutations in the evolution of eyespot number variation**
555 After identifying 10 to 11 regions of the *B. anynana* genome associated with DHEN
556 variation and characterizing the relationship of identified SNPs with nearby genes we
557 observe that the majority of the SNPs fall outside coding sequences (90.8%), and most
558 of the ones that do fall inside protein coding sequences result in synonymous
559 mutations (Supplemental figure/table). Only two genes, BANY.1.2.g01110 (Zinc
560 finger CCCH domain-containing protein 10, *ZC3H10*) and BANY.1.2.g04901
561 (Geranylgeranyl pyrophosphate synthase, *GGPS1*) contain SNPs that represent non-
562 synonymous mutations of unknown effect. Such non-coding DNA variation linked to
563 DHEN is likely to be *cis*-regulatory and controlling the expression of the nearby genes
564 described above. *cis*-regulatory elements are thought to have profound implications
565 in the evolution of morphological diversity (Carroll, 2008). Particularly, they have
566 been associated with variation in pigmentation patterns in a wide variety of animal

567 systems, including the evolution of eggspot pigmentation patterns in cichlids (Santos
568 et al., 2014), wing pigmentation patterns in *Drosophila* (Koshikawa et al., 2015;
569 Werner, Koshikawa, Williams, & Carroll, 2010), divergent pigmentation patterns in
570 capuchino seedeater finches (Campagna et al., 2017), variation in red, black and
571 yellow color patterns in *Heliconius* butterflies due to regulatory changes in the *optix,*
572 *WntA* and *Cortex* genes (Martin & Reed, 2014; Reed et al., 2011; Supple et al., 2013;
573 Van Belleghem et al., 2017) among others. In the case of eyespot number variation,
574 regulatory mutations around the genes identified here might disrupt the reaction-
575 diffusion mechanism of eyespot center differentiation (Connahs et al., 2017 - *bioRxiv*),
576 or later processes of eyespot center signaling, that eventually translate to presence of
577 absence of an eyespot in particular wing sectors.
578
579 Concluding, the genetic variation uncovered in this work affects eyespot number
580 variation on the dorsal surface but not on the ventral surface of the wing. Thus, our
581 work suggests that the genetic variants identified with our analysis affect eyespot
582 number in a surface-specific manner. This surface-specific regulation is potentially
583 mediated via *apA*, a previously identified dorsal eyespot repressor (Prakash &
584 Monteiro, 2018). The polygenic nature of our results argue that genetic variation at
585 the loci identified above, e.g., *Antp, Ubx*, *dpp*, etc, rather than at the *apA* locus itself
586 regulates dorsal eyespot number. The way in which these genes interact is unclear,
587 but changes in gene expression at the identified loci might impact the repression of
588 *apA* in specific wing sectors on the dorsal surface, allowing eyespots to differentiate
589 in those sectors.

590

591 Finally, the use of a genome-wide sequencing strategy allowed us to discover a series
592 of independent loci that appear to contribute to DHEN in *B. anynana*. These loci,
593 predominantly composed of polymorphisms in non-coding DNA, suggest that
594 changes in DHEN are mostly occurring in regions that regulate the expression of
595 previously known eyespot-associated genes. Thus, while our work has enriched the
596 list of genes involved in eyespot number variation, it also confirms that variation at
597 multiple genes, rather than at a single top master regulator or input-output gene
598 (such as *shavenbaby* or *achaete-scute*) is involved in regulating number of serial
599 homologs. This highlights a more complex, but still poorly understood, genetic
600 architecture for serial homolog number regulation.

601

602 **Acknowledgements**

603 We thank Elizabeth Schyling for help rearing families for heritability analysis, and
604 Robert Rak and Chris Bolick for rearing corn plants for the larvae. We also thank the
605 UPR-RP Sequencing and Genomics Facility and the UPR-RP High Performance Computing
606 Facility for additional support in library preparation and computational analysis. This
607 work was funded by a NSF IOS-110382 Doctoral Dissertation Improvement Grant to
608 ELW and AM, a NSF PR-LSAMP Bridge to the Doctorate Program (NSF Grant Award
609 HRD1139888) to AGRC, and a Ministry of Education, Singapore grant (MOE2015-T2-
610 2-159) to AM.

Literature Cited

Axelsson, E., Ratnakumar, A., Arendt, M.-L., Maqbool, K., Webster, M. T., Perloski, M., … Lindblad-Toh, K. (2013). The genomic signature of dog domestication reveals adaptation to a starch-rich diet. *Nature*, *495*(7441), 360–364. https://doi.org/10.1038/nature11837

Baird, N. a., Etter, P. D., Atwood, T. S., Currey, M. C., Shiver, A. L., Lewis, Z. a., … Johnson, E. a. (2008). Rapid SNP Discovery and Genetic Mapping Using Sequenced RAD Markers. *PLoS ONE*, *3*(10), e3376. https://doi.org/10.1371/journal.pone.0003376

Beldade, P., & Brakefield, P. M. (2003). Concerted evolution and developmental integration in modular butterfly wing patterns. *Evolution and Development*, *5*(2), 169–179. https://doi.org/10.1046/j.1525-142X.2003.03025.x

Beldade, P., French, V., & Brakefield, P. M. (2008). Developmental and genetic mechanisms for evolutionary diversification of serial repeats: eyespot size inBicyclus anynana butterflies. *Journal of Experimental Zoology Part B: Molecular and Developmental Evolution*, *310B*(2), 191–201. https://doi.org/10.1002/jez.b.21173

Brakefield, P. M., & French, V. (1993). Butterfly wing patterns. *Acta Biotheoretica*, *41*(4), 447–468. https://doi.org/10.1007/BF00709376

Brakefield, P. M., & van Noordwijk, A. J. (1985). The genetics of spot pattern characters in the meadow brown butterfly Maniola jurtina (Lepidoptera: Satyrinae). *Heredity*, *54*(2), 275–284. https://doi.org/10.1038/hdy.1985.37

Brelsford, A., Toews, D. P. L., & Irwin, D. E. (2017). Admixture mapping in a hybrid zone reveals loci associated with avian feather coloration. *Proc. R. Soc. B*, *284*(1866), 20171106. https://doi.org/10.1098/RSPB.2017.1106

Browning, S. R., & Browning, B. L. (2007). Rapid and Accurate Haplotype Phasing and Missing-Data Inference for Whole-Genome Association Studies By Use of Localized Haplotype Clustering. *The American Journal of Human Genetics*, *81*(5), 1084–1097. https://doi.org/10.1086/521987

Campagna, L., Repenning, M., Silveira, L. F., Fontana, C. S., Tubaro, P. L., & Lovette, I. J. (2017). Repeated divergent selection on pigmentation genes in a rapid finch radiation. *Science Advances*, *3*(5), e1602404. https://doi.org/10.1126/sciadv.1602404

Campbell, C. R., Poelstra, J. W., & Yoder, A. D. (2018). What is Speciation Genomics? The roles of ecology, gene flow, and genomic architecture in the formation of species. *Biological Journal of the Linnean Society*, *124*(4), 561–583. https://doi.org/10.1093/biolinnean/bly063

Carroll, S. B. (2008). Evo-Devo and an Expanding Evolutionary Synthesis: A Genetic Theory of Morphological Evolution. *Cell*, *134*(1), 25–36. https://doi.org/10.1016/j.cell.2008.06.030

Catchen, J. M., Amores, A., Hohenlohe, P. A., Cresko, W. A., Postlethwait, J. H., & De Koning, D.-J. (2011). Stacks: Building and Genotyping Loci De Novo From Short-Read Sequences. *G3: Genes, Genomes, Genetics*, *1*(3), 171–182. https://doi.org/10.1534/g3.111.000240

Catchen, J. M., Hohenlohe, P. A., Bassham, S., Amores, A., & Cresko, W. A. (2013). Stacks: an analysis tool set for population genomics. *Molecular Ecology*, *22*(11), 3124–3140. https://doi.org/10.1111/mec.12354

Cheah, P. Y., Chia, W., & Yang, X. (2000). Jumeaux, a novel Drosophila winged-helix family protein, is required for generating asymmetric sibling neuronal cell fates. *Development*, *127*(15), 3325–3335. Retrieved from http://dev.biologists.org/content/127/15/3325

Cingolani, P., Platts, A., Wang, L. L., Coon, M., Nguyen, T., Wang, L., … Ruden, D. M. (2012). A program for annotating and predicting the effects of single nucleotide polymorphisms, SnpEff. *Fly*, *6*(2), 80–92. https://doi.org/10.4161/fly.19695

Clarke, G. M., Anderson, C. A., Pettersson, F. H., Cardon, L. R., Morris, A. P., & Zondervan, K. T. (2011). Basic statistical analysis in genetic case-control studies. *Nature Protocols*, *6*(2), 121–133. https://doi.org/10.1038/nprot.2010.182

Connahs, H., Tlili, S., van Creij, J., Loo, T. Y. J., Banerjee, T., Saunders, T. E., & Monteiro, A. (2017). Disrupting different Distal-less exons leads to ectopic and missing eyespots accurately modeled by reaction-diffusion mechanisms. *BioRxiv*. https://doi.org/10.1101/183491

Danecek, P., Auton, A., Abecasis, G., Albers, C. A., Banks, E., DePristo, M. A., … Durbin, R. (2011). The variant call format and VCFtools. *Bioinformatics*, *27*(15), 2156–2158.

https://doi.org/10.1093/bioinformatics/btr330

Davey, J. W., Chouteau, M., Barker, S. L., Maroja, L., Baxter, S. W., Simpson, F., … Jiggins, C. D. (2016). Major Improvements to the Heliconius melpomene Genome Assembly Used to Confirm 10 Chromosome Fusion Events in 6 Million Years of Butterfly Evolution. *G3: Genes|Genomes|Genetics*, *6*(3), 695–708. https://doi.org/10.1534/g3.115.023655

Espeland, M., Breinholt, J., Willmott, K. R., Warren, A. D., Vila, R., Toussaint, E. F. A., … Kawahara, A. Y. (2018). A Comprehensive and Dated Phylogenomic Analysis of Butterflies. *Current Biology*, *28*(5), 770–778.e5. https://doi.org/10.1016/j.cub.2018.01.061

Etter, P. D., Bassham, S. L., Hohenlohe, P. A., Johnson, E. a., & Cresko, W. A. (2011). SNP Discovery and Genotyping for Evolutionary Genetics Using RAD Sequencing. *Methods Mol Biol*, *772*(6), 157–178. https://doi.org/10.1007/978-1-61779-228-1

Galant, R., & Carroll, S. B. (2002). Evolution of a transcriptional repression domain in an insect Hox protein. *Nature*, *415*(6874), 910–913. https://doi.org/10.1038/nature717

Garcia-Bellido, A., & de Celis, J. F. (2009). The Complex Tale of the achaete-scute Complex: A Paradigmatic Case in the Analysis of Gene Organization and Function During Development. *Genetics*, *182*(3), 631–639. https://doi.org/10.1534/genetics.109.104083

Holloway, G. J., Brakefield, P. M., & Kofman, S. (1993). The genetics of wing pattern elements in the polyphenic butterfly, Bicyclus anynana. *Heredity*, *70*(2), 179–186. https://doi.org/10.1038/hdy.1993.27

Jombart, T. (2008). adegenet: a R package for the multivariate analysis of genetic markers. *Bioinformatics* , *24*(11), 1403–5. https://doi.org/10.1093/bioinformatics/btn129

Jombart, T., & Ahmed, I. (2011). adegenet 1.3-1: new tools for the analysis of genome-wide SNP data. *Bioinformatics*, *27*(21), 3070–3071. https://doi.org/10.1093/bioinformatics/btr521

Koshikawa, S., Giorgianni, M. W., Vaccaro, K., Kassner, V. A., Yoder, J. H., Werner, T., & Carroll, S. B. (2015). Gain of cis -regulatory activities underlies novel domains of wingless gene expression in Drosophila. *Proceedings of the National Academy of Sciences*, *112*(24), 7524–7529. https://doi.org/10.1073/pnas.1509022112

Kurtz, S., Phillippy, A., Delcher, A. L., Smoot, M., Shumway, M., Antonescu, C., & Salzberg, S. L. (2004). Versatile and open software for comparing large genomes. *Genome Biology*, *5*(2), R12. https://doi.org/10.1186/gb-2004-5-2-r12

Larouche, O., Zelditch, M. L., & Cloutier, R. (2017). Fin modules: an evolutionary perspective on appendage disparity in basal vertebrates. *BMC Biology*, *15*(1), 32. https://doi.org/10.1186/s12915-017-0370-x

Li, H., & Durbin, R. M. (2009). Fast and accurate short read alignment with Burrows-Wheeler transform. *Bioinformatics*, *25*(14), 1754–1760. https://doi.org/10.1093/bioinformatics/btp324

Li, H., Handsaker, B., Wysoker, A., Fennell, T. J., Ruan, J., Homer, N., … Durbin, R. M. (2009). The Sequence Alignment/Map format and SAMtools. *Bioinformatics*, *25*(16), 2078–2079. https://doi.org/10.1093/bioinformatics/btp352

Li, Q., Shen, L., Xin, T., Xiang, W., Chen, W., Gao, Y., … Li, M. (2009). Role of Scrib and Dlg in anterior-posterior patterning of the follicular epithelium during Drosophila oogenesis. *BMC Developmental Biology*, *9*(1), 60. https://doi.org/10.1186/1471-213X-9-60

Marcellini, S., & Simpson, P. (2006). Two or Four Bristles: Functional Evolution of an Enhancer of scute in Drosophilidae. *PLoS Biology*, *4*(12), e386. https://doi.org/10.1371/journal.pbio.0040386

Martin, A., & Reed, R. D. (2014). Wnt signaling underlies evolution and development of the butterfly wing pattern symmetry systems. *Developmental Biology*, *395*(2), 367–378. https://doi.org/10.1016/j.ydbio.2014.08.031

McGregor, A. P., Orgogozo, V., Delon, I., Zanet, J., Srinivasan, D. G., Payre, F., & Stern, D. L. (2007). Morphological evolution through multiple cis-regulatory mutations at a single gene. *Nature*, *448*(7153), 587–590. https://doi.org/10.1038/nature05988

McKenna, A., Hanna, M., Banks, E., Sivachenko, A., Cibulskis, K., Kernytsky, A., … DePristo, M. A. (2010). The Genome Analysis Toolkit: A MapReduce framework for analyzing next-generation DNA sequencing data. *Genome Research*, *20*(9), 1297–1303. https://doi.org/10.1101/gr.107524.110

719 Montague, M. J., Li, G., Gandolfi, B., Khan, R., Aken, B. L., Searle, S. M. J., … Warren, W. C. (2014).
720 Comparative analysis of the domestic cat genome reveals genetic signatures underlying feline
721 biology and domestication. *Proceedings of the National Academy of Sciences*, *111*(48), 17230–
722 17235. https://doi.org/10.1073/pnas.1410083111
723 Monteiro, A., Brakefield, P. M., & French, V. (1994). The evolutionary genetics and developmental
724 basis of wing pattern variation in the butterfly Bicyclus anynana. *Evolution*, *48*(4), 1147–1157.
725 https://doi.org/10.2307/2410374
726 Monteiro, A., Brakefield, P. M., & French, V. (1997). Butterfly eyespots: the genetics and development
727 of the color rings. *Evolution*. Retrieved from http://www.jstor.org/stable/2411050
728 Monteiro, A., Chen, B., Ramos, D. M., Oliver, J. C., Tong, X., Guo, M., … Kamal, F. (2013). Distal-less
729 regulates eyespot patterns and melanization in Bicyclus butterflies. *Journal of Experimental*
730 *Zoology Part B: Molecular and Developmental Evolution*, *320*(5), 321–331.
731 https://doi.org/10.1002/jez.b.22503
732 Monteiro, A., Chen, B., Scott, L. C., Vedder, L., Prijs, H. J., Belicha-Villanueva, A., & Brakefield, P. M.
733 (2007). The combined effect of two mutations that alter serially homologous color pattern
734 elements on the fore and hindwings of a butterfly. *BMC Genetics*, *8*, 22.
735 https://doi.org/10.1186/1471-2156-8-22
736 Monteiro, A., Glaser, G., Stockslager, S., Glansdorp, N., & Ramos, D. M. (2006). Comparative insights
737 into questions of lepidopteran wing pattern homology. *BMC Developmental Biology*, *6*(1), 52.
738 https://doi.org/10.1186/1471-213X-6-52
739 Monteiro, A., Prijs, J., Bax, M., Hakkaart, T., & Brakefield, P. M. (2003). Mutants highlight the modular
740 control of butterfly eyespot patterns. *Evolution and Development*, *5*(2), 180–187.
741 https://doi.org/10.1046/j.1525-142X.2003.03029.x
742 Nadeau, N. J., Ruiz, M., Salazar, P., Counterman, B. A., Medina, J. A., Ortiz-Zuazaga, H., … Papa, R.
743 (2014). Population genomics of parallel hybrid zones in the mimetic butterflies, H. melpomene
744 and H. erato. *Genome Research*, *24*(8), 1316–1333. https://doi.org/10.1101/gr.169292.113
745 Narum, S. R., Buerkle, C. A., Davey, J. W., Miller, M. R., & Hohenlohe, P. A. (2013). Genotyping-by-
746 sequencing in ecological and conservation genomics. *Molecular Ecology*, *22*(11), 2841–2847.
747 https://doi.org/10.1111/mec.12350
748 Nowell, R. W., Elsworth, B., Oostra, V., Zwaan, B. J., Wheat, C. W., Saastamoinen, M., … Blaxter, M.
749 (2017). A high-coverage draft genome of the mycalesine butterfly Bicyclus anynana.
750 *GigaScience*. https://doi.org/10.1093/gigascience/gix035
751 Ohde, T., Yaginuma, T., & Niimi, T. (2013). Insect Morphological Diversification Through the
752 Modification of Wing Serial Homologs. *Science*, *340*(6131), 495–498.
753 https://doi.org/10.1126/science.1234219
754 Oliver, J. C., Beaulieu, J. M., Gall, L. F., Piel, W. H., & Monteiro, A. (2014). Nymphalid eyespot serial
755 homologues originate as a few individualized modules. *Proceedings of the Royal Society B:*
756 *Biological Sciences*, *281*(1787), 20133262–20133262. https://doi.org/10.1098/rspb.2013.3262
757 Oliver, J. C., Tong, X., Gall, L. F., Piel, W. H., & Monteiro, A. (2012). A Single Origin for Nymphalid
758 Butterfly Eyespots Followed by Widespread Loss of Associated Gene Expression. *PLoS Genetics*,
759 *8*(8). https://doi.org/10.1371/journal.pgen.1002893
760 Owen, D. (1993). Spot variation in Maniola jurtina (L.) (Lepidoptera: Satyridae) in southern Portugal
761 and a comparison with the Canary Islands. *Biological Journal of the Linnean Society*, *49*(4), 355–
762 365. https://doi.org/10.1006/bijl.1993.1041
763 Özsu, N., & Monteiro, A. (2017). Wound healing, calcium signaling, and other novel pathways are
764 associated with the formation of butterfly eyespots. *BMC Genomics*, *18*(1), 788.
765 https://doi.org/10.1186/s12864-017-4175-7
766 Payre, F., Vincent, A., & Carreno, S. (1999). ovo/svb integrates Wingless and DER pathways to control
767 epidermis differentiation. *Nature*, *400*(6741), 271–275. https://doi.org/10.1038/22330
768 Prakash, A., & Monteiro, A. (2018). apterous A specifies dorsal wing patterns and sexual traits in
769 butterflies. *Proceedings of the Royal Society of London B: Biological Sciences*, *285*(1873).
770 https://doi.org/10.1098/rspb.2017.2685
771 Purcell, S., Neale, B., Todd-Brown, K., Thomas, L., Ferreira, M. A. R., Bender, D., … Sham, P. C. (2007).
772 PLINK: A Tool Set for Whole-Genome Association and Population-Based Linkage Analyses. *The*
773 *American Journal of Human Genetics*, *81*(3), 559–575. https://doi.org/10.1086/519795

774 Reed, R. D., Papa, R., Martin, A., Hines, H. M., Counterman, B. A., Pardo-Diaz, C., … McMillan, W. O.
775 (2011). optix Drives the Repeated Convergent Evolution of Butterfly Wing Pattern Mimicry.
776 *Science*, *333*(6046), 1137–1141. https://doi.org/10.1126/science.1208227
777 Reed, R. D., & Serfas, M. S. (2004). Butterfly Wing Pattern Evolution Is Associated with Changes in a
778 Notch/Distal-less Temporal Pattern Formation Process. *Current Biology*, *14*(13), 1159–1166.
779 https://doi.org/10.1016/j.cub.2004.06.046
780 Rellstab, C., Gugerli, F., Eckert, A. J., Hancock, A. M., & Holderegger, R. (2015). A practical guide to
781 environmental association analysis in landscape genomics. *Molecular Ecology*, *24*(17), 4348–
782 4370. https://doi.org/10.1111/mec.13322
783 Rochette, N. C., & Catchen, J. M. (2017). Deriving genotypes from RAD-seq short-read data using
784 Stacks. *Nature Protocols*, *12*(12), 2640–2659. https://doi.org/10.1038/nprot.2017.123
785 Ronshaugen, M., McGinnis, N., & McGinnis, W. (2002). Hox protein mutation and macroevolution of
786 the insect body plan. *Nature*, *415*, 914. https://doi.org/10.0.4.14/nature716
787 Ruvinsky, I., & Gibson-Brown, J. J. (2000). Genetic and developmental bases of serial homology in
788 vertebrate limb evolution. *Development*, *127*(24), 5233 LP-5244. Retrieved from
789 http://dev.biologists.org/content/127/24/5233.abstract
790 Saenko, S. V., Marialva, M. S., & Beldade, P. (2011). Involvement of the conserved Hox gene
791 Antennapedia in the development and evolution of a novel trait. *EvoDevo*, *2*(1), 9.
792 https://doi.org/10.1186/2041-9139-2-9
793 Santos, M. E., Braasch, I., Boileau, N., Meyer, B. S., Sauteur, L., Böhne, A., … Salzburger, W. (2014). The
794 evolution of cichlid fish egg-spots is linked with a cis-regulatory change. *Nature*
795 *Communications*, *5*, 5149. https://doi.org/10.1038/ncomms6149
796 Schachat, S. R., Oliver, J. C., & Monteiro, A. (2015). Nymphalid eyespots are co-opted to novel wing
797 locations following a similar pattern in independent lineages. *BMC Evolutionary Biology*, *15*(1),
798 20. https://doi.org/10.1186/s12862-015-0300-x
799 Stern, D. L., & Orgogozo, V. (2008). THE LOCI OF EVOLUTION: HOW PREDICTABLE IS GENETIC
800 EVOLUTION? *Evolution*, *62*(9), 2155–2177. https://doi.org/10.1111/j.1558-5646.2008.00450.x
801 Supple, M. A., Hines, H. M., Dasmahapatra, K. K., Lewis, J. J., Nielsen, D. M., Lavoie, C., … Counterman, B.
802 A. (2013). Genomic architecture of adaptive color pattern divergence and convergence in
803 Heliconius butterflies. *Genome Research*, *23*(8), 1248–1257.
804 https://doi.org/10.1101/gr.150615.112
805 Tien, A.-C., Rajan, A., Schulze, K. L., Ryoo, H. D., Acar, M., Steller, H., & Bellen, H. J. (2008). Ero1L, a thiol
806 oxidase, is required for Notch signaling through cysteine bridge formation of the Lin12-Notch
807 repeats in Drosophila melanogaster. *The Journal of Cell Biology*, *182*(6), 1113–1125.
808 https://doi.org/10.1083/jcb.200805001
809 Tokita, C. K., Oliver, J. C., & Monteiro, A. (2013). A Survey of Eyespot Sexual Dimorphism across
810 Nymphalid Butterflies. *International Journal of Evolutionary Biology*, *2013*, 1–6.
811 https://doi.org/10.1155/2013/926702
812 Tomoyasu, Y., Wheeler, S. R., & Denell, R. E. (2005). Ultrabithorax is required for membranous wing
813 identity in the beetle Tribolium castaneum. *Nature*, *433*(7026), 643–647.
814 https://doi.org/10.1038/nature03272
815 Tong, X., Hrycaj, S., Podlaha, O., Popadić, A., & Monteiro, A. (2014). Over-expression of Ultrabithorax
816 alters embryonic body plan and wing patterns in the butterfly Bicyclus anynana. *Developmental*
817 *Biology*, *394*(2), 357–366. https://doi.org/10.1016/j.ydbio.2014.08.020
818 Van Belleghem, S. M., Rastas, P., Papanicolaou, A., Martin, S. H., Arias, C. F., Supple, M. A., … Papa, R.
819 (2017). Complex modular architecture around a simple toolkit of wing pattern genes. *Nature*
820 *Ecology & Evolution*, *1*, 0052. https://doi.org/10.1038/s41559-016-0052
821 Weatherbee, S. D., Frederik Nijhout, H., Grunert, L. W., Halder, G., Galant, R., Selegue, J., & Carroll, S.
822 (1999). Ultrabithorax function in butterfly wings and the evolution of insect wing patterns.
823 *Current Biology*, *9*(3), 109–115. https://doi.org/10.1016/S0960-9822(99)80064-5
824 Werner, T., Koshikawa, S., Williams, T. M., & Carroll, S. B. (2010). Generation of a novel wing colour
825 pattern by the Wingless morphogen. *Nature*, *464*(7292), 1143–1148.
826 https://doi.org/10.1038/nature08896
827 Westerman, E. L., Chirathivat, N., Schyling, E., & Monteiro, A. (2014). Mate preference for a
828 phenotypically plastic trait is learned, and may facilitate preference-phenotype matching.

Evolution, *68*(6), 1661–1670. https://doi.org/10.1111/evo.12381

Westerman, E. L., Monteiro, A., Sherry, D., Hoshooley, J., Snell-Rood, E., Davidowitz, G., … Rutowski, R. (2016). Rearing Temperature Influences Adult Response to Changes in Mating Status. *PLOS ONE*, *11*(2), e0146546. https://doi.org/10.1371/journal.pone.0146546

Yamamoto-Hino, M., & Goto, S. (2016). Spätzle-Processing Enzyme-independent Activation of the Toll Pathway in *Drosophila* Innate Immunity. *Cell Structure and Function*, *41*(1), 55–60. https://doi.org/10.1247/csf.16002

Table legends

Table 1. DHEN is heritable. Summary DHEN data for offspring from 6 families each of 0x0, 1x1, and 2x2 DHEN crosses, separated by sex. Offspring with asymmetric DHEN are included in the average DHEN estimate.

Table 2. DHEN candidate genes. BANY.1.2 gene ID, gene name, molecular function, biological process, BANY.1.2 scaffold ID all refer to the *B. anynana* v1.2 genome assembly and annotation (Nowell et al., 2017).

847 **Figure legends**

848

849 **Figure 1. Eyespot pattern and number variation in *Bicyclus anynana.*** (A) Eyespot
850 pattern on the ventral side of wings: forewing displays two eyespots; hindwing
851 displays seven eyespots. (B) Eyespots pattern on dorsal side of wings. Male (left)
852 displaying two dorsal forewing eyespots and zero dorsal hindwing eyespots and
853 female displaying two dorsal forewing eyespots and three dorsal hindwing eyespots.
854 (C) Dorsal hindwing eyespot number (DHEN) variation, ranging from zero to five UV-
855 reflective spots, marked by white arrows (i–vi).

856

857 **Figure 2. Genome-wide population structure and linkage disequilibrium (LD)**
858 **in the study population**. **(A.)** Principal Component Analysis (PCA) of the allelic
859 variation observed in 5000 randomly-selected genome-wide SNPs in the study
860 population across both phenotype groups, DHE presence (*pre*, red) and DHE absence
861 (*abs,* blue). Ellipses display boundaries of the 95% confidence interval. Little
862 contribution to variation in the principal components and overlap of the variation on
863 both phenotype groups suggests lack of underlying demographic substructuring in
864 the study population. **(B.)** Genome-wide linkage disequilibrium (LD) in the *B.*
865 *anynana* study population. Grey dots represent LD values for a SNP pairwise
866 comparison. In red, Loess regression smoothed curve representing LD decay. Insert:
867 Zoomed-in LD decay curve, indicating distance at which LD is halved (465,570 bp)
868 and corresponding r^2 value (0.137).

869

Figure 3. Genome-wide association with dorsal hindwing eyespot number. (A.) Plots show genomic association to dorsal hindwing eyespot number (top) and F_{ST} between individuals with different dorsal hindwing eyespot numbers (bottom). Each dot represents a single SNP. Dashed lines represent the threshold for detecting a significant genome-wide association (top, in red) and F_{ST} (bottom, in blue). Scaffolds containing both significant association and F_{ST} outliers are marked with asterisks. **(B.)** Genomic scaffolds from the *Bicyclus_anynana*_v1x2 genome are arranged along the 21 chromosomes of the *Heliconius melpomene* v2 assembly. For ordering the *B. anynana* scaffolds along the *H. melpomene* genome, only matches with a minimum percentage of identity of 90% and a minimum alignment length of 200 bp were used. If scaffolds matched multiple *H. melpomene* chromosomes, the scaffold was positioned along the chromosome to which it had the most matches. Using this strategy 76.7% of the *B. anynana* genome scaffolds were aligned to the *H. melpomene* genome.

Figure 4. Zoom-in on putative genomic regions underlying dorsal hindwing eyespot number variation. Plots show genomic association to dorsal hindwing eyespot number (top) and F_{ST} (bottom) between individuals with different dorsal hindwing eyespot numbers for scaffolds with significant outliers (red for association and blue for F_{ST}). Each dot represents a single SNP. Green and red lines show matches of the *B. anynana* scaffolds (minimum percentage of identity of 70% and a minimum alignment length of 150 bp) to the *H. melpomene* v2 assembly. Green lines represent the most frequent matches of the scaffold to a *H. melpomene* chromosome, whereas

893 red lines represent matches to a different *H. melpomene* chromosome. Vertical black
894 rectangles represent gene models. Gene models in red represent genes that have
895 previously been demonstrated to be involved in eye spot development.

Table 1: DHEN is heritable. Summary DHEN data for offspring from 6 families each of 0x0, 1x1, and 2x2 DHEN crosses, separated by sex. Offspring with asymmetric DHEN are included in the average DHEN estimate.

	0 x 0 DHEN Families		**1 x 1 DHEN Families**		**2 x 2 DHEN Families**	
	Females	Males	Females	Males	Females	Males
0 DHEN	46	159	2	47	0	14
1 DHEN	55	15	45	36	19	38
2 DHEN	24	2	43	9	67	27
3 DHEN	2	0	4	0	6	0
Average DHEN	**0.87**	**0.17**	**1.49**	**0.63**	**1.87**	**1.13**

Table 2: DHEN candidate genes. BANY.1.2 gene ID, gene name, molecular function, biological process, BANY.1.2 scaffold ID all refer to the *B. anynana* v1.2 genome assembly and annotation (Nowell et al., 2017).

BANY.1.2 gene ID	Gene name	Gene description	BANY.1.2 scaffold ID	Known candidate
g00030	*CDase*	Neutral ceramidase	BANY00001	Yes (Özsu & Monteiro, 2017)
g00647	*PIK3AP1*	Phosphoinositide 3-kinase adapter protein 1	BANY00004	No
g00653	*dpp*	Protein decapentaplegic	BANY00004	Yes (Connahs et al., 2017 - *bioRxiv*)
g00658	*dlg1*	Disks large 1 tumor suppressor protein	BANY00004	Yes (Cheah, Chia, & Yang, 2000; Q. Li et al., 2009; Tien et al., 2008)
g00659	*cmk-1*	Calcium/calmodulin-dependent protein kinase type 1	BANY00004	No
g00681	*numb*	Protein numb	BANY00004	Yes (Cheah, Chia, & Yang, 2000; Q. Li et al., 2009; Tien et al., 2008)
g01110	*ZC3H10*	Zinc finger CCCH domain-containing protein 10	BANY00007	No
g02571	*Antp*	Homeotic protein antennapedia	BANY00019	Yes (Saenko, Marialva, & Beldade, 2011)
g02579	*Ubx*	Homeotic protein ultrabithorax	BANY00019	Yes (Weatherbee 1999; Tomoyasu et al. 2005; Tong et al. 2014)
g04715	*C2CD5*	C2 domain-containing protein 5	BANY00042	No
g04901	*GGPS1*	Geranylgeranyl pyrophosphate synthase	BANY00044	No
g04904	*slo*	Calcium-activated potassium channel slowpoke	BANY00044	No
g04910	*spz*	Protein spaetzle	BANY00044	No
g05412	*pyx*	Transient receptor potential channel pyrexia	BANY00052	No
g10819	*Ero1L*	Ero1-like protein	BANY00148	Yes (Cheah, Chia, & Yang, 2000; Q. Li et al., 2009; Tien et al., 2008)

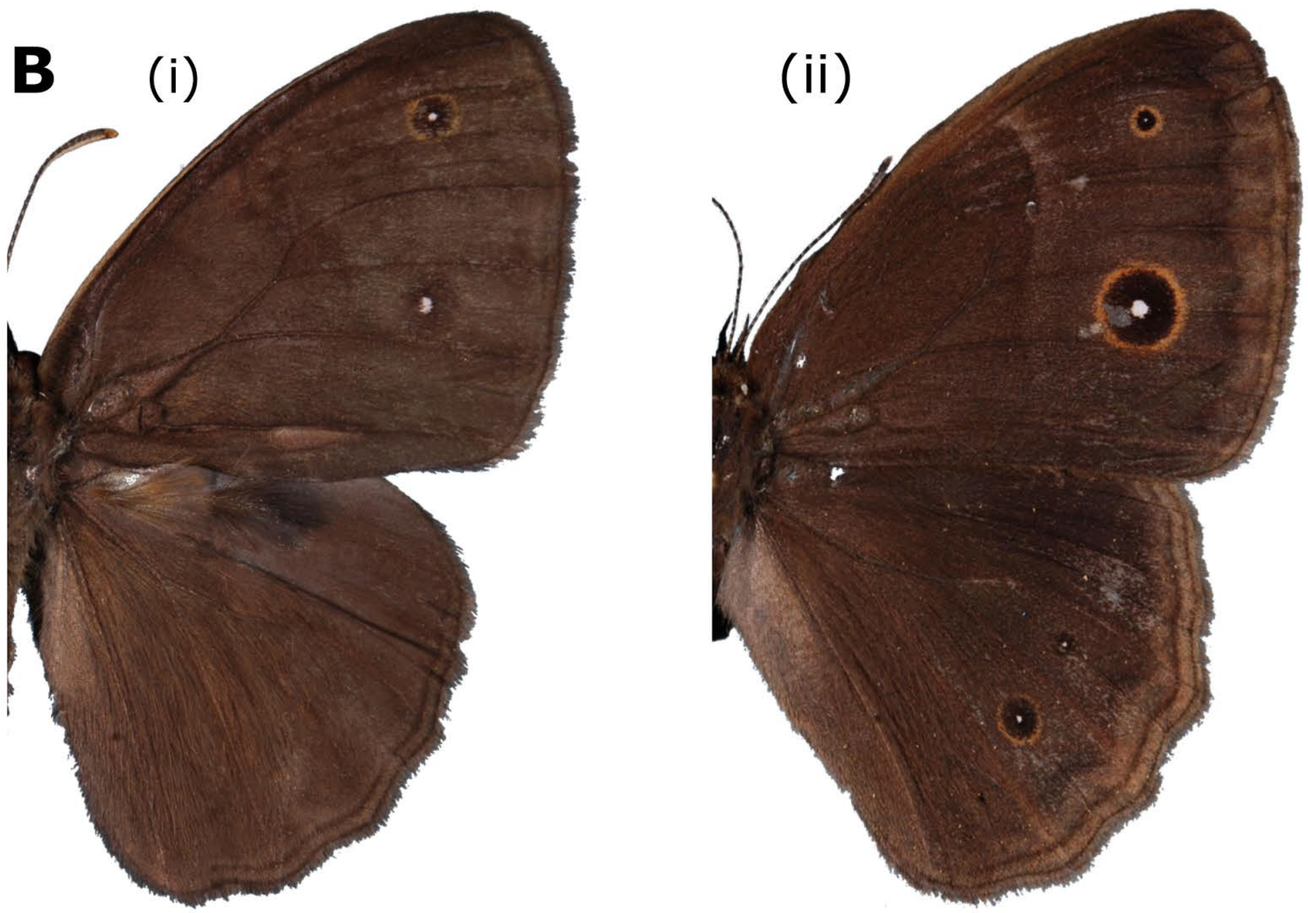

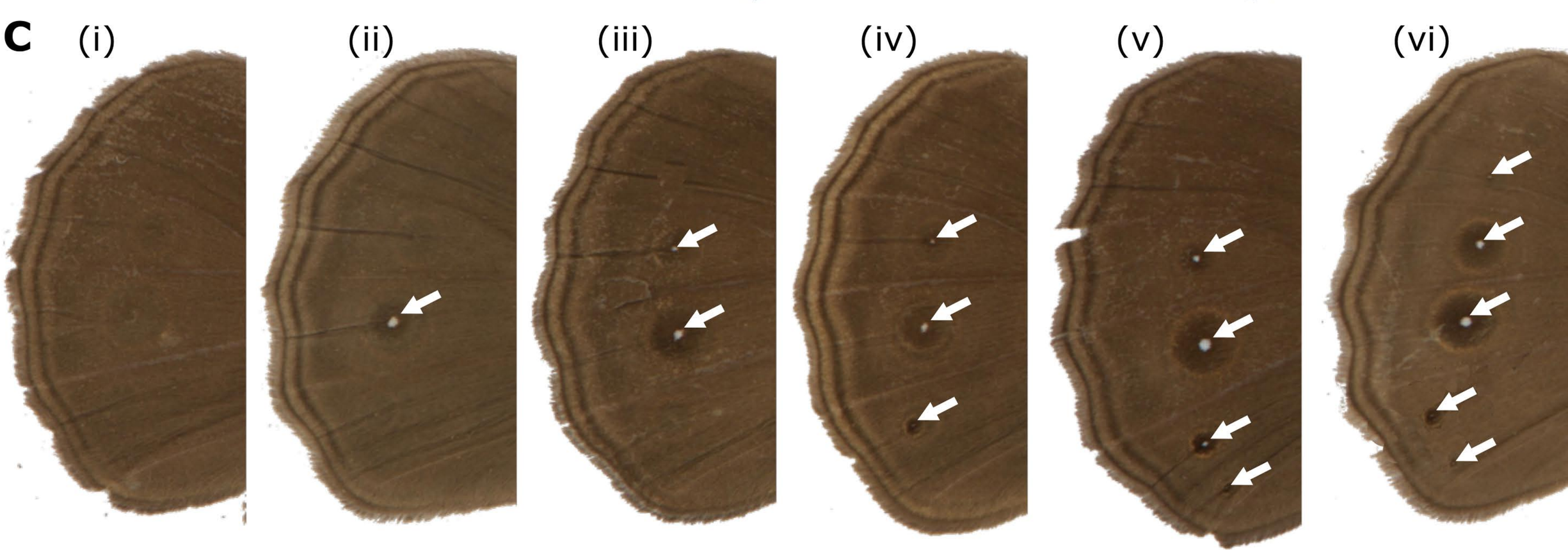

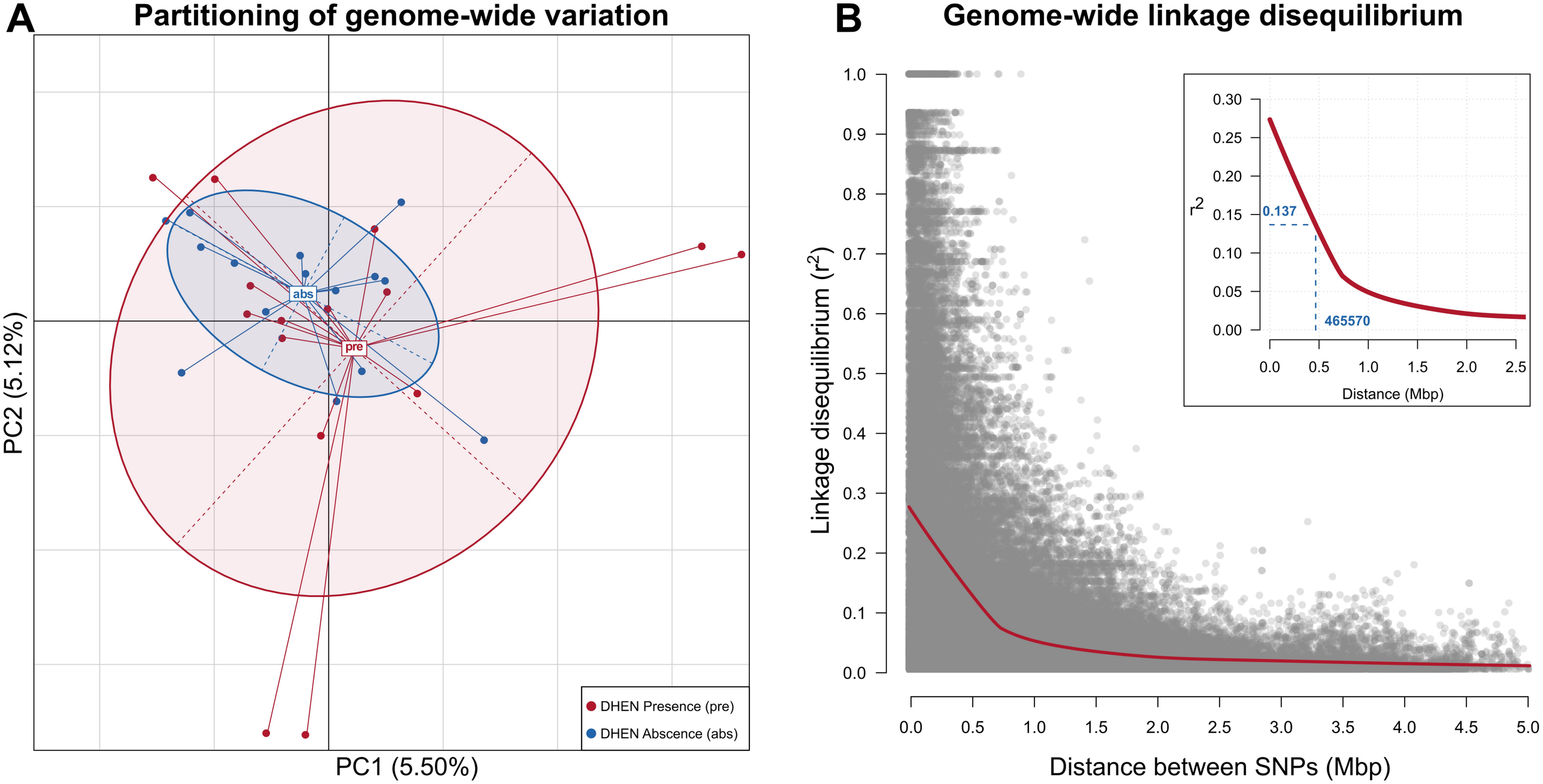
A
Partitioning of genome-wide variation
abs
pre
PC2 (5.12%)
PC1 (5.50%)
DHEN Presence (pre)
DHEN Abscence (abs)
B
Genome-wide linkage disequilibrium
Linkage disequilibrium (r2)
1.0
0.9
0.8
0.7
0.6
0.5
0.4
0.3
0.2
0.1
0.0
0.0
0.5
1.0
1.5
2.0
2.5
3.0
3.5
4.0
4.5
5.0
Distance between SNPs (Mbp)
r2
0.30
0.25
0.20
0.15
0.10
0.05
0.00
0.137
465570
0.0
0.5
1.0
1.5
2.0
2.5
Distance (Mbp)

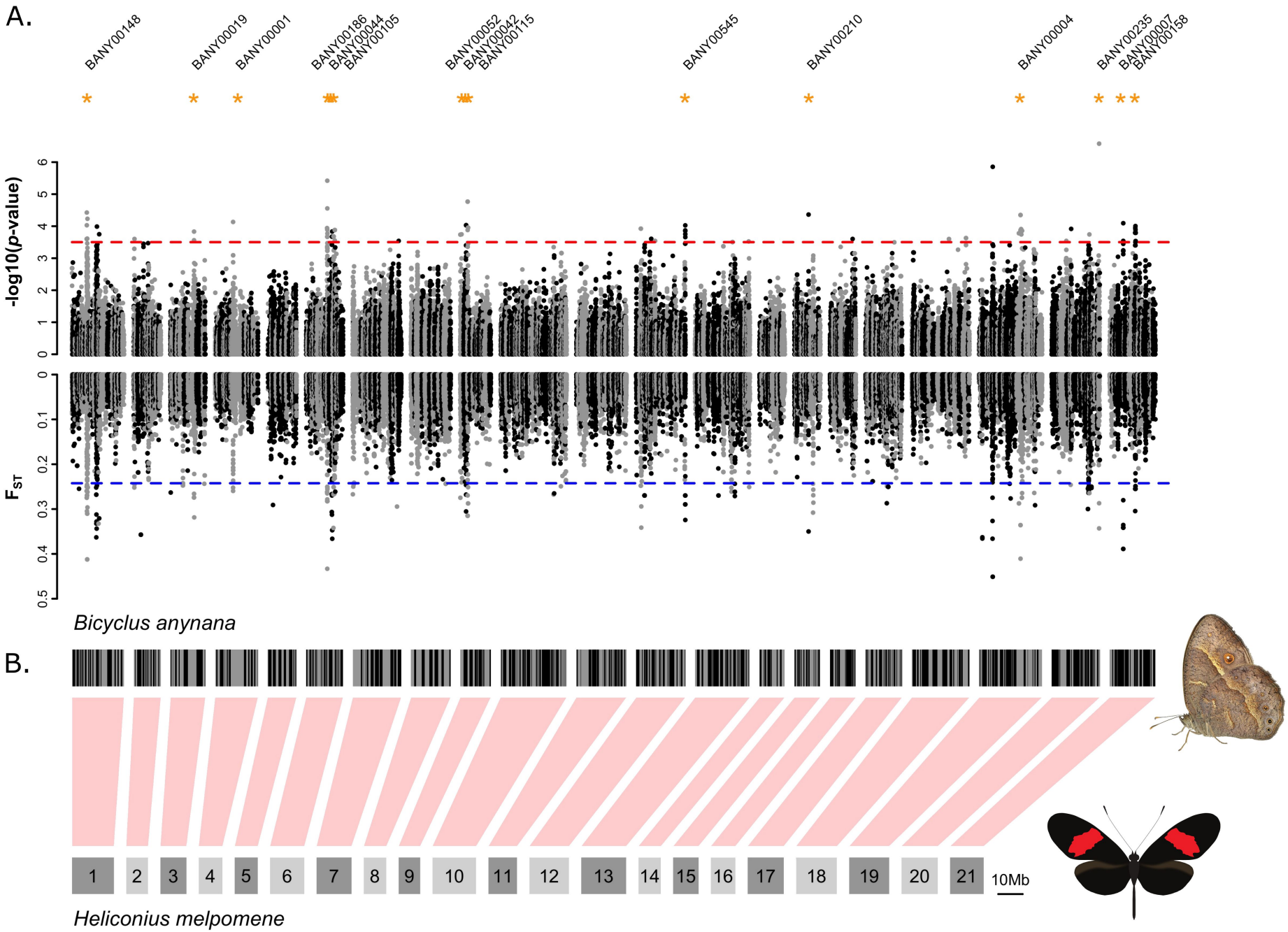
A.
BANY00148
BANY00019
BANY00001
BANY00186
BANY00044
BANY00105
BANY00052
BANY00042
BANY00115
BANY00545
BANY00210
BANY00004
BANY00235
BANY00007
BANY00158
-log10(p-value)
0
1
2
3
4
5
6
FST
0
0.1
0.2
0.3
0.4
0.5
Bicyclus anynana
B.
1
2
3
4
5
6
7
8
9
10
11
12
13
14
15
16
17
18
19
20
21
10Mb
Heliconius melpomene

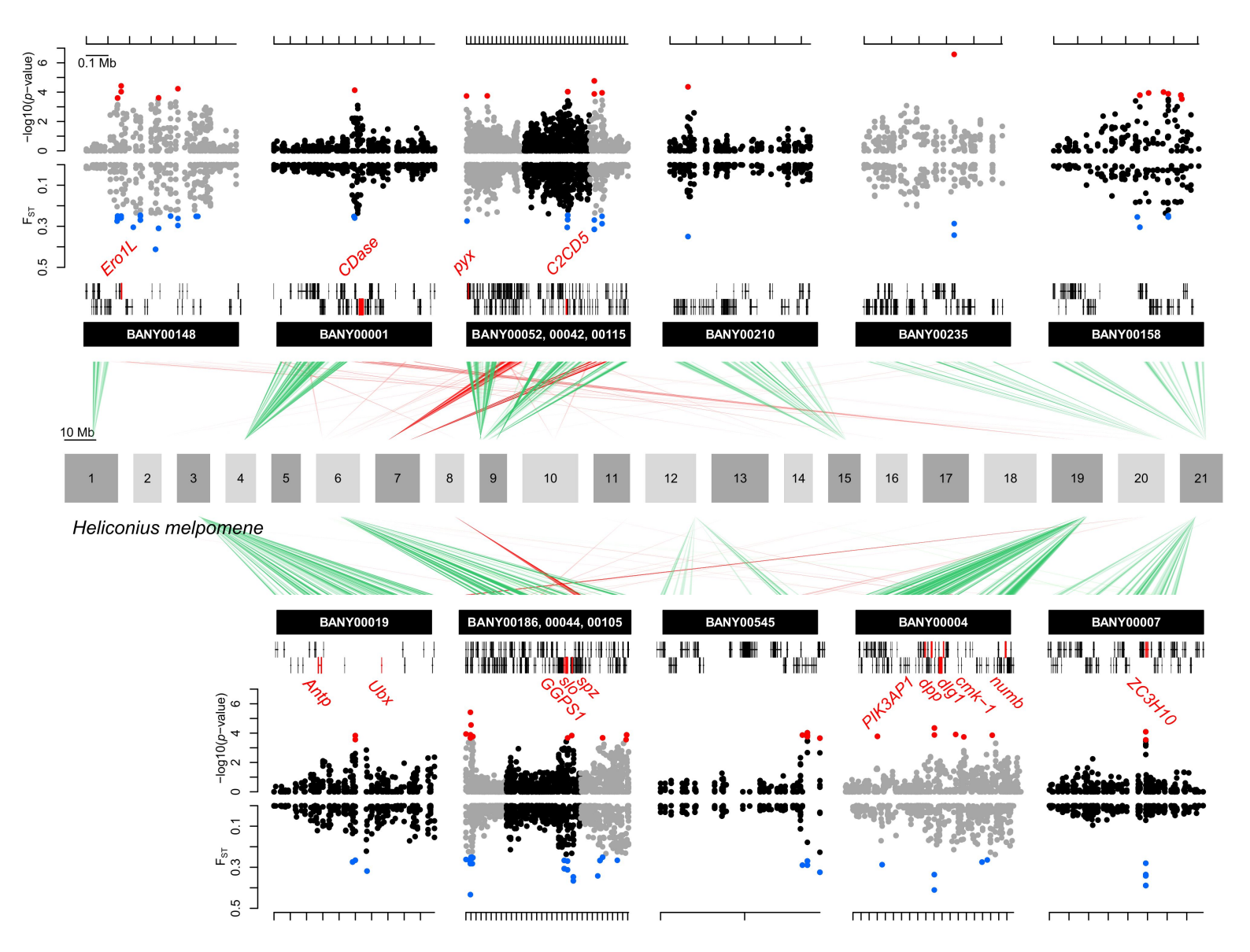
0.1 Mb
−log10(p−value)
0
2
4
6
FST
0.1
0.3
0.5
Ero1L
CDase
pyx
C2CD5
BANY00148
BANY00001
BANY00052, 00042, 00115
BANY00210
BANY00235
BANY00158
10 Mb
1
2
3
4
5
6
7
8
9
10
11
12
13
14
15
16
17
18
19
20
21
Heliconius melpomene
BANY00019
BANY00186, 00044, 00105
BANY00545
BANY00004
BANY00007
Antp
Ubx
spz
slo
GGPS1
PIK3AP1
dpp
dlg1
cmk−1
numb
ZC3H10